Click Here for Full Article

Intra-seasonal variability of polar mesospheric clouds due to inter-hemispheric coupling

B. Karlsson,[1] C. E. Randall,[1,2] S. Benze,[1] M. Mills,[1] V. L. Harvey,[1] S. M. Bailey,[3] and J. M. Russell III[4]

Received 3 August 2009; revised 15 September 2009; accepted 21 September 2009; published 24 October 2009.

[1] Polar mesospheric cloud (PMC) observations have revealed that interannual variability near the polar summer mesopause can be forced by planetary wave activity in the winter stratosphere. We use data from the Aeronomy of Ice in the Mesosphere (AIM) satellite to investigate coupling between the Arctic winter stratosphere and PMC variability in the Antarctic summer of 2007–2008. We find a high correlation between zonal mean PMC frequency and Arctic winter zonal mean winds from the Goddard Earth Observing System, as well as Microwave Limb Sounder zonal mean temperatures. The time lag between changes in the winter stratosphere and the connected response in PMCs varies from 2 to 8 days. We suggest that the differences in lag times are related to the evolution of cloud altitudes throughout the season. The results here are the first to show evidence for intra-seasonal PMC variability forced by inter-hemispheric coupling. **Citation:** Karlsson, B., C. E. Randall, S. Benze, M. Mills, V. L. Harvey, S. M. Bailey, and J. M. Russell III (2009), Intra-seasonal variability of polar mesospheric clouds due to inter-hemispheric coupling, *Geophys. Res. Lett.*, *36*, L20802, doi:10.1029/2009GL040348.

1. Introduction

[2] Polar Mesospheric Clouds (PMCs), the highest clouds in the Earth's atmosphere, are formed in the cold polar summer mesopause region. Observations show that there are significant hemispheric differences in PMC morphology: the occurrence frequency is higher in the northern hemisphere (NH) than in the southern hemisphere (SH) [*Bailey et al.*, 2005], PMCs are brighter in the NH [*DeLand et al.*, 2006] and their variability (both inter- and intra-seasonal) is greater in the SH [*Bailey et al.*, 2007]. *Karlsson et al.* [2007] showed that the year-to-year variation in PMC particle radii is related to planetary wave (PW) activity in the winter troposphere and stratosphere. In addition, they suggested that the asymmetry in PW activity between the two hemispheres could explain the differences between the NH and SH PMCs, with the more dynamically active NH winter troposphere contributing to more PMC variability observed in the SH. This inter-hemispheric connection was first indicated and discussed in model simulations by *Becker et al.* [2004] and *Becker and Fritts* [2006]. *Karlsson et al.* [2009, hereafter K09], studied the mechanism behind the coupling using the Canadian Middle Atmosphere Model (CMAM). They found a statistically significant day-to-day correlation between the vertical component of the Eliassen-Palm flux in the winter lower stratosphere and the temperature at the summer mesopause, from which altitude-dependent lag times were derived using correlation analyses.

[3] In this work we discuss the influence of the winter stratosphere on the intra-seasonal PMC variability during the SH 2007–2008 season. Aeronomy of Ice in the Mesosphere (AIM) PMC observations [*Russell et al.*, 2009] are interpreted in the context of global temperatures from the NASA Microwave Limb Sounder (MLS) [*Schwartz et al.*, 2008] and zonal winds from the Goddard Earth Observing System (GEOS-5) [*Reinecker et al.*, 2008]. We find that the intra-seasonal signatures observed in the PMC data can be traced back to the dynamical conditions in the winter stratosphere with lag times between 2 and 8 days. We associate the differences in lag times with the PMC altitude shift within the season.

2. Inter-hemispheric Coupling

[4] The global mean meridional circulation in the mesosphere is driven primarily by gravity waves (GWs). The background zonal wind (U) in the stratosphere dictates which part of the GW spectrum propagates to the mesosphere [*Lindzen*, 1981]. In the summer hemisphere the stratospheric U is easterly, so GWs with eastward phase speeds can propagate to the mesosphere and break, inducing equatorward flow. By continuity, this mesospheric meridional circulation causes upward motion that cools air adiabatically in the high latitude summer mesosphere. In the winter hemisphere, the stratospheric U is westerly, so waves with westward phase speeds propagate up to the mesosphere and break, inducing poleward and downward flow. As the air descends it adiabatically heats the lower polar winter mesosphere. From 70–90 km, the mean circulation is characterized by meridional flow from the summer pole to the winter pole.

[5] Filtering of GWs by the background zonal flow is the fundamental mechanism for inter-hemispheric coupling. Changes in U caused largely by PWs in the lower atmosphere generate variations in the mesospheric GW drag and consequently alter the mesospheric meridional flow. In the summer stratosphere PWs, having a westward phase speed relative to the mean zonal flow, cannot propagate vertically. Thus, the summer stratosphere remains calm. High PW activity in the winter troposphere and stratosphere, however,

[1]Laboratory for Atmospheric and Space Physics, University of Colorado at Boulder, Boulder, Colorado, USA.
[2]Also at Atmospheric and Oceanic Sciences, University of Colorado at Boulder, Boulder, Colorado, USA.
[3]Bradley Department of Electrical Computer and Engineering, Virginia Polytechnic Institute and State University, Blacksburg, Virginia, USA.
[4]Center for Atmospheric Sciences, Hampton University, Hampton, Virginia, USA.

Copyright 2009 by the American Geophysical Union.
0094-8276/09/2009GL040348$05.00

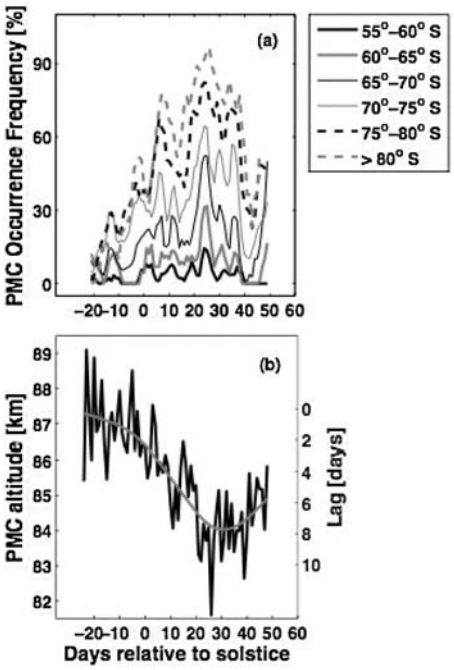

Figure 1. AIM PMC observations: (a) CIPS PMC occurrence frequencies in 5° latitude bins versus days relative to solstice and (b) SOFIE PMC mean peak altitude versus days relative to solstice. The gray smooth curve illustrates the mean peak altitude change in time.

causes the high-latitude stratosphere and low-latitude mesosphere to experience warming, while the high-latitude mesosphere and low-latitude stratosphere experience cooling. This quadrupole structure can be explained as follows: PWs decelerate U, leading to a net reduction of the net GW drag that drives the mesospheric meridional circulation [*Becker et al.*, 2004]. As a result the winter mesospheric meridional flow weakens, reducing the adiabatic heating at high latitudes. Thus, the high-latitude winter mesosphere is anomalously cooler than average during events of high PW activity in the lower atmosphere. By continuity, the weaker poleward mass flux in the winter mesosphere will also result in reduced upwelling in the equatorial mesosphere, and thus a warming in the temperature (T) anomaly field. In the winter stratosphere, the PWs give rise to an enhanced Brewer-Dobson circulation, thus warming the high latitudes and cooling the equatorial region. This quadrupole response in the temperature field is reversed for events of low PW activity (K09).

[6] The upper part of the equatorial T anomaly response is suggested to be the 'carrier' of the signal from the winter hemisphere to the summer mesopause (K09). Briefly, changes in T in the low latitude mesosphere lead to changes in the T gradient between lower and higher latitudes in the summer mesosphere. Via thermal wind balance such a change in the T gradient induces a change in U in the summer mesosphere. In response, GW drag and thus the equatorward mesospheric meridional flow in the summer mesosphere is modified (K09; H. Körnich et al., manuscript in preparation, 2009). In turn, the temperature, and possibly the supply of water and condensation nuclei, in the polar summer mesosphere is altered, affecting the formation and properties of PMCs. Following these arguments, an anomalously warmer (cooler) winter stratosphere with high (low) PW activity will be associated with an anomalously warm (cool) summer mesopause and thus fewer (more) and dimmer (brighter) clouds.

[7] K09 found a systematic increase in the time lag between wintertime PW activity and the response at decreasing altitudes in the summer mesosphere, and associated this with a GW drag - U feedback similar to that which occurs in the QBO [*Campbell and Shepherd*, 2005]. The altitude dependence of the response is crucial for the study presented here.

3. Method

[8] The AIM Cloud Imaging and Particle Size (CIPS) instrument [*McClintock et al.*, 2009] is a 4-camera panoramic UV nadir imager operating at 265 nm that measures scattered sunlight. We analyze measurements from the sunward pointing "PX" camera, which observes forward scattering and is thus most sensitive to PMCs. The PMC detection algorithm is described by *Benze et al.* [2009]. Figure 1a shows PMC occurrence frequencies averaged over 5° latitude bins from 55° – 85°S during the SH 2007–2008 summer. During this time, large variability in PMC frequency is observed at all latitudes. PMC detections have higher signal-to-noise at high latitudes where PMCs are brighter, so only PMC frequencies poleward of 70°S are used for this study. The data series ends abruptly at day 50, when AIM went into a temporary safehold.

[9] The AIM Solar Occultation For Ice Experiment (SOFIE) measures ice extinction profiles with a vertical resolution of ∼1–2 km [e.g., *Gordley et al.*, 2009; *Hervig et al.*, 2009]. Figure 1b shows the PMC peak ice extinction altitude at 3.064 μm; PMCs descend from ∼87 km in early Dec to ∼84 km in late Jan.

[10] MLS temperatures [*Schwartz et al.*, 2008] are used to investigate inter-hemispheric coupling signatures. The vertical resolution is ∼8 km at 1 hPa and ∼9 km at 0.1 hPa. In addition, we use zonal mean wind data from the GEOS-5 data assimilation system [*Reinecker et al.*, 2008]. The GEOS-5 analyses extend to ∼80 km, but observations are assimilated only in the stratosphere, so uncertainties are larger in the mesosphere.

4. Results and Discussion

[11] Figure 2 illustrates the different dynamical activity in the winter and summer stratosphere as well as the connection to the summer mesosphere. Daily zonal mean U, averaged over potential temperatures (θ) from 800–1200 K (∼10–5 hPa) and 59.75–61.25° latitude, is shown for both hemispheres, along with PMC frequency averaged poleward of 70° S during the 2007–2008 SH summer. At a latitude of ∼60°, this altitude region is a good indicator of the variability in the winter stratosphere. The same region is chosen in the summer hemisphere for comparison. It is obvious from Figure 2 that U in the NH (winter) stratosphere is much more variable than in the SH (summer). Note also the similarity in the PMC variability and the NH U. In Dec (dashed box in 2a), the PMC frequency, shifted back in time by 2 days, co-varies with the winter strato-

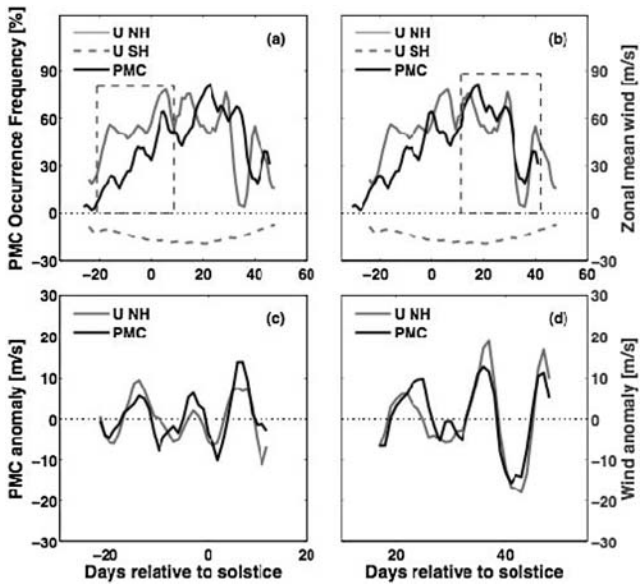

Figure 2. (a) Zonal wind, U, averaged over 59.75 – 61.25 °N and 800 – 1200 K (solid gray), U at 60°S and 5 hPa (dashed gray) and SH PMC frequency, poleward of 70 °S, shifted 2 days backward. (b) Same as Figure 2a but for a 7-day shift backward. (c) Low-frequency filtered data from the box in Figure 2a. (d) Low-frequency filtered data from the box in Figure 2b.

spheric U. In Jan (Figure 2b, dashed box) highest correlations are found when the PMC data is shifted 7 days backward in time relative to the NH U.

[12] In order to investigate the correlation between the winter U and PMC variability during these two parts of the season, the two data sets must be 'de-seasonalized', since the overall seasonal variability will otherwise comprise a significant part of the correlation. We accomplish this by removing the low frequency variability, which we derive by applying a Hodrick-Prescott filter with a smoothing factor of $\lambda = 300$ [*Hodrick and Prescott*, 1997]. Henceforth in this paper, the filtered data sets are referred to as "anomalies" associated with "day-to-day" variations, rather than with changes occurring due to seasonality. Figures 2c and 2d show the PMC and winter U anomalies within each of the boxes in Figures 2a and 2b. At the 99% confidence level, the correlation coefficient between PMC frequency and NH U in Figure 2c (Figure 2d) is 0.74 (0.91), based on 35 (31) data points.

[13] As mentioned in Section 1 and 2, K09 noted that the time lag of the inter-hemispheric coupling signal had an altitude dependence for which the lag increased with decreasing altitudes in the summer hemisphere. This provides an explanation for the differences in lag time inferred from the correlations in Figure 2. As seen in Figure 1b, the clouds are ~3 km higher in Dec than in Jan. Since higher altitudes respond first to inter-hemispheric coupling, the lag is shorter early in the PMC season. This is in qualitative agreement with the altitude dependence of the lag time seen in the CMAM study (K09). In order to quantify this, we now establish a simple relationship between the lag time and the PMC altitude, based on the SOFIE observations of PMC altitude in Figure 1b and the time lag analysis in Figure 2. CIPS PMC occurrence frequency responds to the NH U with a lag increasing from 2 days when the average PMC altitude is 86.5 km (early season) to 7 days when the PMC average altitude is 84.35 km (late season). This suggests that the signal propagates approximately 2.25 km in 5 days, or 0.45 km/day. Assuming a linearly downward propagating signal this results in the relationship

$$lag(z) = \frac{(z_0 - z)}{0.45\ ^{\mathrm{km}}/_{\mathrm{day}}} \quad (1)$$

with $z_0 = 87.5$; this equation applies to $z<z_0$, where the lag is positive. The smoothed altitude dependence of the lag in the cloud occurrence frequency is illustrated as the solid gray curve in Figure 1b. We now combine this dependence with equation (1) to smoothly shift the PMC data set in time before performing the correlation with the NH U data set. The result of this adjustment is shown in Figure 3. Pearson's correlation coefficient between variations in U and the lag-adjusted PMC frequency is 0.84 at a 99% level of significance calculated from the anomaly data in Figure 3b. The significance level was determined using moving block bootstrapping for various block lengths between 5 and 30 days to account for the possible serial dependence in both time series.

[14] Finally, we examine the correlation with the global U and T fields. Figure 4 illustrates on a global scale the correlations between the PMC occurrence frequency anomaly, U anomaly field and T anomaly field from day −25 to day 49. The black contours in Figure 4 denote the ±0.6 and ±0.7 correlation coefficients (r). The areas in the summer mesosphere and lower thermosphere and in the winter stratosphere where $|r|>0.6$ are significant within the 99% level; areas of high correlation in the winter mesosphere are significant within the 95% level using a block length of 10. Shown in Figures 4a and 4b are the instantaneous PMC – U and PMC – T correlations. As seen in Figure 4a, there is no strong instantaneous correlation between the PMC and the U field. In Figure 4b, a strong anti-correlation is present in the area where the clouds exist, at SH high latitudes between 75 km and 90 km. This is to be expected since temperature is one of the driving forces in PMC formation and growth. The positive correlation at altitudes above the PMCs is related to the reversed meridional flow in the thermosphere, which leads to descent and adiabatic heating

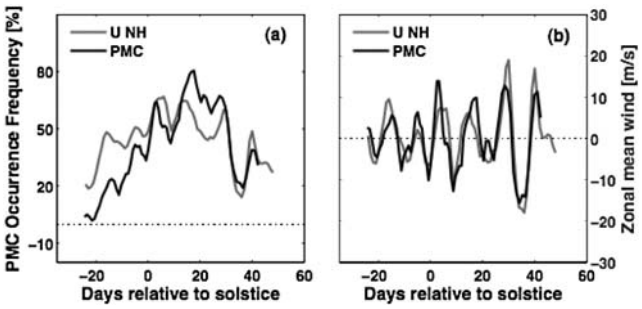

Figure 3. (a) U averaged over 59.75 – 61.25 °N and 800–1200 K (solid gray) and lag adjusted PMC frequency. (b) Same as Figure 3a but the low-frequency variability is removed.

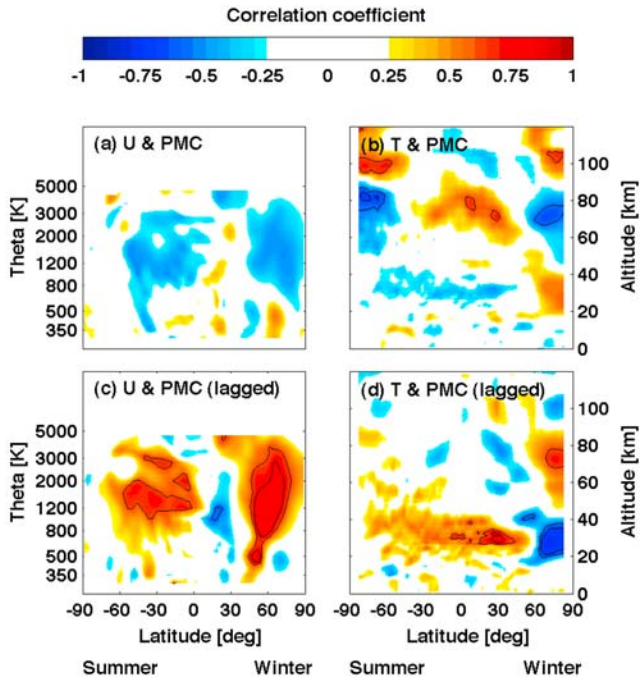

Figure 4. PMC anomaly correlated with (a) the U anomaly field and (b) the T anomaly field, without any lag. (c and d) Same as Figures 4a and 4b but for the lag adjusted PMC anomaly.

above the PMCs. There are also regions of alternating positive and negative correlations in the NH polar mesosphere and thermosphere; this is discussed below. Note that the MLS data has large uncertainties above $\sim$ 95 km [*Schwartz et al.*, 2008] and should thus be interpreted with caution.

[15] In Figures 4c and 4d the PMC anomaly is adjusted to compensate for the shift in PMC altitude over the course of the season. Large areas of positive correlation with the U field are now visible, with stronger correlations in the NH winter. The positive correlation between winter stratospheric U and PMC occurrence frequency is in agreement with the inter-hemispheric coupling mechanism described in Section 2. The high correlation between PMCs and U in the summer hemisphere is due to dynamics in the winter stratosphere affecting the summer stratospheric flow. This correlation was also noticed by K09, but was ruled out as a possible source of the variability in the mesopause region; the U changes in the summer are simply too small to significantly change the gravity wave fluxes from below. Unfortunately, correlations with U in the mesosphere, where the coupling occurs, are hampered by either scarce or inaccurate U data.

[16] As seen in Figure 4d, lag-adjusted PMC – T correlations show parts of the quadrupole structure discussed in Section 2. The negative correlation in the high-latitude stratosphere and the positive correlation in the equatorial region agree well with results from previous studies [*Karlsson et al.*, 2007; K09]. Thus, this analysis shows that the strongest correlations between day-to-day variability in PMCs and T occur at lower altitudes in the opposite (winter) hemisphere between 2 and 8 days earlier.

[17] Figure 4b showed that PMC variability is also strongly correlated with T in the winter mesosphere without a lag-adjustment. We speculate that this correlation is due to the fact that both PMCs and winter mesospheric T respond to changes in planetary wave activity in the lower atmosphere, but with different lag times. Thus, we argue that day-to-day variability in PMCs originates from variability in the winter stratosphere a few days earlier, as illustrated by the strong correlation signatures in Figures 4c and 4d, rather than from instantaneous variability in the winter mesosphere (4a and 4b).

5. Conclusions

[18] We have linked the intra-seasonal variability in the 2007–2008 SH summer PMC season to variability in the NH winter stratosphere. This inter-hemispheric coupling should be particularly clear in intra-seasonal PMC fluctuations when the winter hemisphere exhibits large variability, such as the NH 2007–2008 winter.

[19] Propagation of the signal from the winter stratosphere to the summer mesopause region requires several days; more time is required to propagate to lower summertime altitudes. We suggest that the observed time lag varies over the season because clouds exist at different altitudes at different times, but that the lag at a fixed altitude is relatively constant. This is qualitatively supported by the CMAM study (K09).

[20] **Acknowledgments.** This work was supported by NASA's Small Explorers Program under contract NAS5-03132 and by NSF CEDAR grant ATM0737705.

References

Bailey, S. M., A. W. Merkel, G. E. Thomas, and J. N. Carstens (2005), Observations of polar mesospheric clouds by the Student Nitric Oxide Explorer, *J. Geophys. Res.*, *110*, D13203, doi:10.1029/2004JD005422.

Bailey, S. M., A. W. Merkel, G. E. Thomas, and D. W. Rusch (2007), Hemispheric differences in polar mesospheric cloud morphology observed by the Student Nitric Oxide Explorer, *J. Atmos. Sol. Terr. Phys.*, *69*, 1407–1418, doi:10.1016/j.jastp.2007.02.008.

Becker, E., and D. C. Fritts (2006), Enhanced gravity-wave activity and interhemispheric coupling during the MaCWAVE/MIDAS northern summer program 2002, *Ann. Geophys.*, *24*, 1175–1188.

Becker, E., A. Müllemann, F.-J. Lübken, H. Körnich, P. Hoffmann, and M. Rapp (2004), High Rossby-wave activity in austral winter 2002: Modulation of the general circulation of the MLT during the MaCWAVE/MIDAS northern summer program, *Geophys. Res. Lett.*, *31*, L24S03, doi:10.1029/2004GL019615.

Benze, S., et al. (2009), Comparison of polar mesospheric cloud measurements from the cloud imaging and particle size experiment and the solar backscatter ultraviolet instrument in 2007, *J. Atmos. Sol. Terr. Phys.*, *71*, 365–372, doi:10.1016/j.jastp.2008.07.014.

Campbell, L. J., and T. G. Shepherd (2005), Constraints on wave drag parameterization schemes for simulating the quasibiennial oscillation. Part I: Gravity wave forcing, *J. Atmos. Sci.*, *62*, 4178–4195, doi:10.1175/JAS3616.1.

DeLand, M. T., E. P. Shettle, G. E. Thomas, and J. J. Olivero (2006), A quarter-century of satellite polar mesospheric cloud observations, *J. Atmos. Sol. Terr. Phys.*, *68*, 9–29, doi:10.1016/j.jastp.2005.08.003.

Gordley, L. L., et al. (2009), The solar occultation for ice experiment, *J. Atmos. Sol. Terr. Phys.*, *71*, 300–315, doi:10.1016/j.jastp.2008.07.012.

Hervig, M. E., L. Gordley, M. Stevens, J. Russell III, S. Bailey, and G. Baumgarten (2009), Interpretation of SOFIE PMC measurements: Cloud identification and derivation of mass density, particle shape, and particle size, *J. Atmos. Sol. Terr. Phys.*, *71*, 316–330, doi:10.1016/j.jastp.2008.07.009.

Hodrick, R. J., and E. C. Prescott (1997), Postwar U.S. business cycles: An empirical investigation, *J. Money Credit Banking*, *29*, 1–16, doi:10.2307/2953682.

Karlsson, B., H. Körnich, and J. Gumbel (2007), Evidence for interhemispheric stratosphere-mesosphere coupling derived from noctilucent cloud properties, *Geophys. Res. Lett.*, *34*, L16806, doi:10.1029/2007GL030282.

Karlsson, B., C. McLandress, and T. G. Shepherd (2009), Inter-hemispheric mesospheric coupling in a comprehensive middle atmosphere model, *J. Atmos. Sol. Terr. Phys.*, *71*, 518–530, doi:10.1016/j.jastp.2008.08.006.

Lindzen, R. S. (1981), Turbulence and stress due to gravity wave and tidal breakdown, *J. Geophys. Res.*, *86*, 9707–9714, doi:10.1029/JC086iC10p09707.

McClintock, W. E., et al. (2009), The cloud imaging and particle size experiment on the Aeronomy of Ice in the Mesosphere mission: Instrument concept, design, calibration, and on-orbit performance, *J. Atmos. Sol. Terr. Phys.*, *71*, 340–355, doi:10.1016/j.jastp.2008.10.011.

Reinecker, M. M., et al. (2008), The GEOS-5 data assimilation system—Documentation of versions 5.0.1 and 5.1.0, *NASA Tech Rep. TM-2007-104606*, vol. 27, 92 pp.

Russell, J. M., III, et al. (2009), The Aeronomy of Ice in the Mesosphere (AIM) mission: Overview and early science results, *J. Atmos. Sol. Terr. Phys.*, *71*, 289–299, doi:10.1016/j.jastp.2008.08.011.

Schwartz, M. J., et al. (2008), Validation of the Aura Microwave Limb Sounder temperature and geopotential height measurements, *J. Geophys. Res.*, *113*, D15S11, doi:10.1029/2007JD008783.

S. M. Bailey, Bradley Department of Electrical Computer and Engineering, Virginia Polytechnic Institute and State University, Blacksburg, VA 24061, USA.

S. Benze, V. L. Harvey, B. Karlsson, M. Mills, and C. E. Randall, Laboratory for Atmospheric and Space Physics, University of Colorado at Boulder, Boulder, CO 80305-0000, USA. (bodil.karlsson@lasp.colorado.edu)

J. M. Russell III, Center for Atmospheric Sciences, Hampton University, Hampton, VA 23668, USA.